A Critical Analysis of the α, β and γ Phases in Poly (vinylidene fluoride) Using FTIR

Xiaomei Cai[1], Tingping Lei[*,2,3], Daoheng Sun[4], and Liwei Lin[4,5]

[1]*School of Science, Jimei University, Xiamen 361021, China*

[2]*Fujian Key Laboratory of Special Energy Manufacturing, Huaqiao University, Xiamen 361021, China*

[3]*College of Mechanical Engineering and Automation, Huaqiao University, Xiamen 361021, China*

[4]*School of Aerospace Engineering, Xiamen University, Xiamen 361005, China*

[5]*Department of Mechanical Engineering, University of California, Berkeley, California 94720, USA*

[*]**Corresponding author:** tplei@hqu.edu.cn

I. FTIR and XRD spectra of spin coated membranes

Fig. S1 presents IR spectra and XRD patterns of spin coated membranes dried in air and with/without experiencing further stretching process. It is found that samples of different phase (α, β or γ) domination can be obtained by controlling the solution concentration, rotating speed and the post treatment of stretching, as evidenced by the absorbance bands and diffraction peaks shown in the corresponding IR spectra and XRD patterns, respectively.

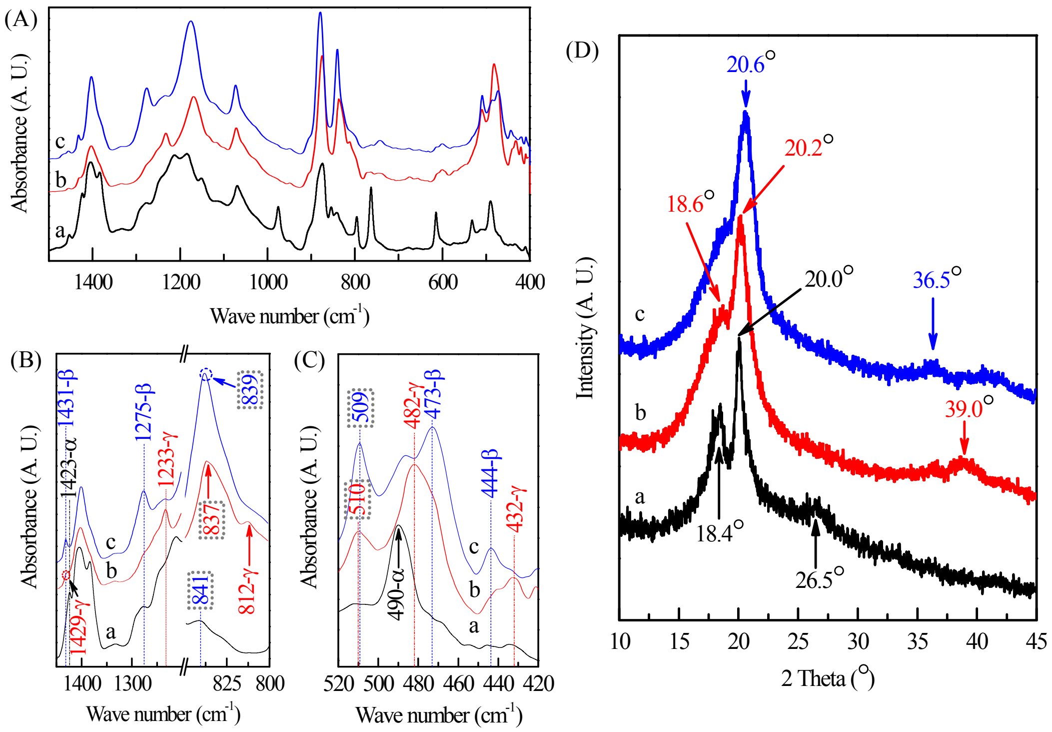

Fig. S1. FTIR spectra (A-C) and XRD patterns (D) of membranes spin coated from PVDF solutions with $V_{\mathrm{NMP}}/V_{\mathrm{acetone}}$ at 5/5: curve 'a' for the sample from 8 wt% PVDF at a rotation speed of 2000 rpm; curve 'b' for the sample from 12 wt% PVDF at a rotation speed of 5000 rpm; curve 'c' for stretching of sample (b) drawn at 80 °C with a ratio of 4.

II. Determination of *F*(β)/*F*(γ)

In order to determine a preferable method for the calculation of F(β)/F(γ), peak area ratio (PAR), peak height ratio (PHR) and peak height difference ratio (PHDR) of the two bands around at 1275 and 1234 cm^{-1}, and integrated area ratio (IAR) of deconvoluted curves centered around at 840 cm^{-1} band [1], were calculated on seven samples, including five samples with the mixture of β/γ and two respectively dominated by β and γ phases, as mentioned in the main article (**Fig. S2)**. The values from PAR and PHR modes are calculated based on automatic baseline correction of the above two bands in peak area and height tools of OMNIC software, respectively. The peak height difference in PHDR mode, namely, the height differences (absorbance differences) between the peaks around at 1275 and 1234 cm^{-1} and their nearest valleys, is shown in inset in **Fig. S2**. The integrated area ratio (IAR) of deconvoluted curves centered around at 840 cm^{-1} band is demonstrated in **Fig. S3**. The values of F(β)/F(γ) for these seven samples calculated based on four different calculation modes are listed in **Tab. S1**.

It is easy to observe that all the values from IAR calculation are bigger than 1, which is very inappropriate for sample 1# (curve ‘a’ in **Fig. S2)** that is obviously dominated by γ phase. On the other hand, since sample 1# is dominated by γ phase, a calculated F(β)/F(γ) value of 0.11 (calculated from PHDR) is probably much better than 0.66 and 0.65(calculated from PAR and PHR, respectively). Similarly, in sample 7# (curve ‘g’ in **Fig. S2)** where β phase is rather dominant, a value of 17.80 may be much better than 9.25 and 9.18. In addition, in sample 6# (curve ‘f’ in **Fig. S2**) a ratio of 0.78 (smaller than 1) calculated from PHDR may be much better than higher ratios of 1.79 and 1.76 (bigger than 1) respectively from PAR and PHR, since in sample 6# the 481 cm^{-1} band is very close to the γ-phase exclusive band of 482 cm^{-1} (an intensive band exclusive to γ phase). According to some prior literatures [2-4] and the present manuscript, it is easy to find that the 1234 and 482 cm^{-1} bands are the two most intensive absorption peaks exclusive to γ phase. As such, in sample 6# the fraction of β phase, F(β), should be lower than that of γ phase, F(γ). Therefore, it is reasonable to state that PHDR mode is the most preferable for the calculation of F(β)/F(γ).

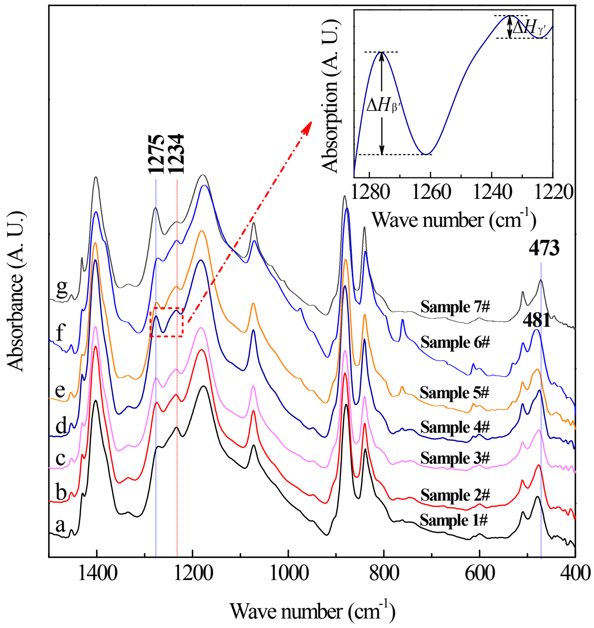

Fig. S2 FTIR spectra of electrospun samples duplicated from the main article: Samples 1#, 2#, 3# and 4# corresponding to curves ‘a’ , ‘b’, ‘c’ and ‘d’ in Fig. 6, samples 5# and 6# corresponding to curves ‘c’ and ‘d’ in Fig. 5, and sample 7# corresponding to curve ‘c’ in Fig. 3(C), respectively.

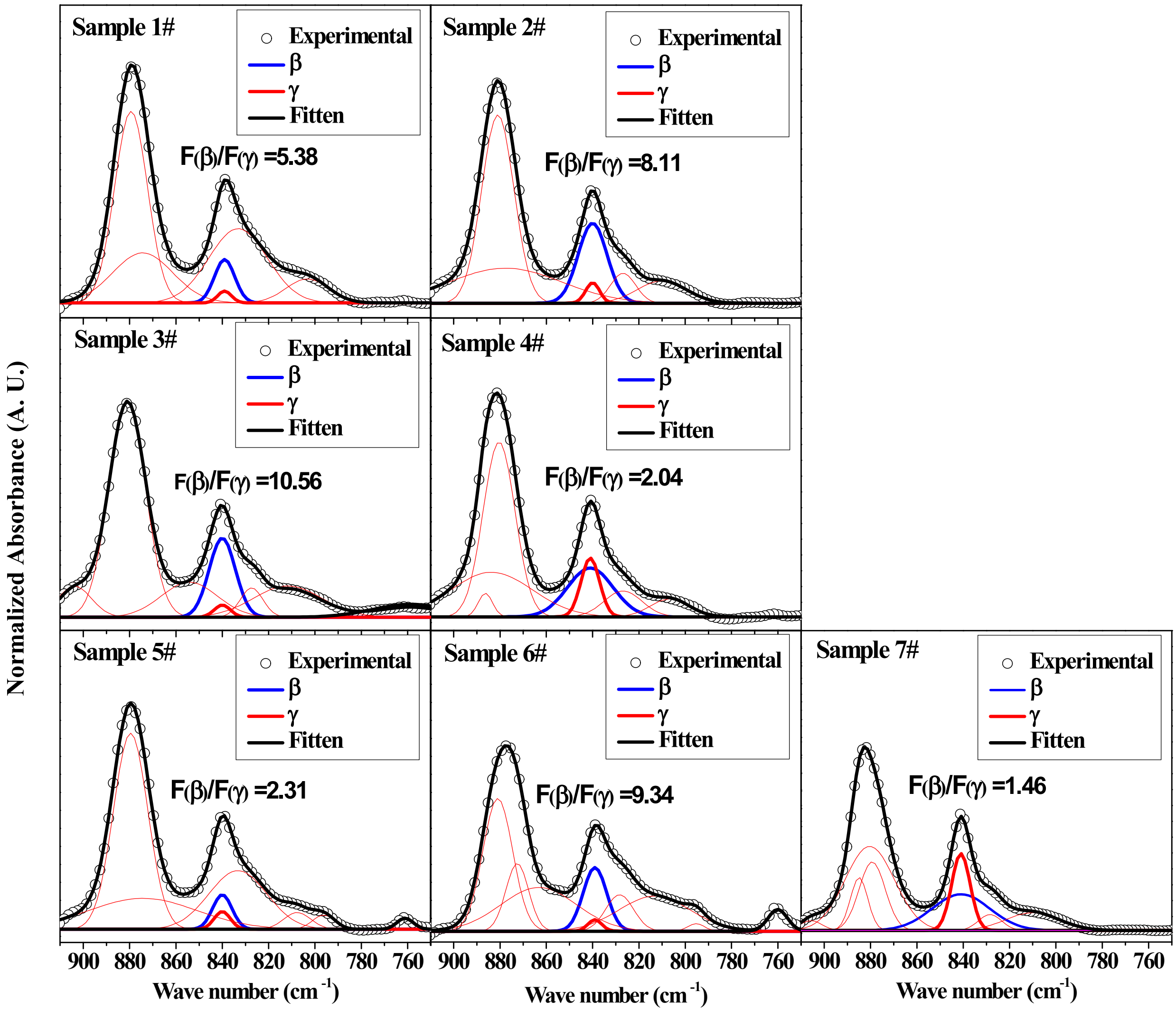

Fig. S3 Curve deconvolution of FTIR spectra in 750-910 cm^{-1} range of the samples shown in Fig. S2. The open circles are experimental data and the solid from the best curve fit. The fitting peak centered at 840 cm^{-1} for electroactive β and γ phases are highlighted in blue and red and the ratio of *F*(β) and *F*(γ) are mentioned in the inset.

Tab. S1 Values of *F*(β)/*F*(γ) for samples in **Fig. S2** based on four different calculation modes

Calculation modes	*F*(β)/*F*(γ)						
	Sample 1#	Sample 2#	Sample 3#	Sample 4#	Sample 5#	Sample 6#	Sample 7#
PAR	0.66	2.13	2.45	3.46	2.34	1.79	9.25
PHR	0.65	2.14	2.43	3.48	2.30	1.76	9.18
IAR	5.38	8.11	10.56	2.04	2.31	9.34	1.46
PHDR	0.11	1.29	2.06	4.02	1.96	0.78	17.80

To further prove the PHDR mode is the most preferable for the calculation of F(β)/F(γ), another four electrospun samples with the mixture of β/γ phases were investigated, as shown in **Fig. S4**(A). PVDF solution of 12 wt% with $V_{NMP}/V_{acetone}$ at 5/5 was electrospun at a constant flow rate of 500 μL/h and either the applied voltage on the needle tip or the tip-to-collector distance (working distance) was changed. It is known that "effective stretching" during the electrospinning is the main cause for α→β transformation [5-6]; therefore by using a low voltage such as 4.5 kV (Sample I, curve ‘a’) or a high voltage like 10.5 kV (Sample II, curve ‘b’), or a small working distance such as 4 cm (Sample III, curve ‘c’) or a big working distance like 20 cm (Sample IV, curve ‘d’), effective stretching will be reduced and more γ phase would be therefore produced as evidenced by the strong or medium absorption at peaks around 1234 and 480 cm^{-1}. The calculated F(β)/F(γ) based on PAR, PHR and PHDR methods is presented in **Fig. S4**(B). The ratios F(β)/F(γ) based on PAR and PHR methods are very close and almost approximates 1 or are bigger than 1, while a smaller value (normally less than 1) was calculated for each sample when using PHDR method. For example, in Sample III the γ phase is very dominant; however, values of 0.99 and 0.98 were calculated for F(β)/F(γ) when PAR and PHR methods were respectively used, which should be rather inappropriate. Therefore, it is clear that our proposal using the PHDR method is much more preferable to the PAR and PHR methods.

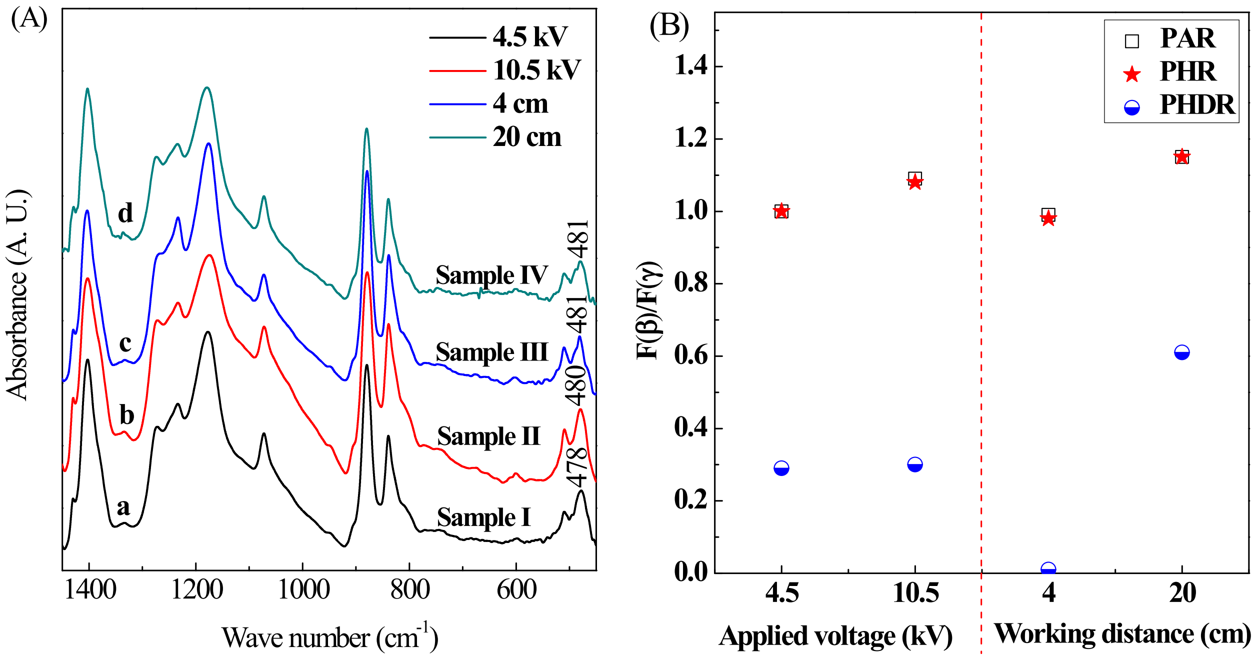

Fig. S4 (A) FTIR spectra of electrospun samples with mixture of β/γ phases prepared from 12 wt% PVDF with $V_{NMP}/V_{acetone}$ at 5/5 and at a constant flow rate of 500 μL/h, either by changing the applied voltage (4.5 and 10.5 kV for samples I and II, respectively) or working distance (4 and 20 cm for samples III and IV, respectively); (B) ratios of F(β)/F(γ) calculated from PAR, PHR and PHDR methods

III. Percentages of the α, β and γ phases

Although the crystalline content in typical PVDF samples is no more than 50 - 60%, calculation of the relative content of each phase in terms of crystalline components, especially the content of the electroactive β phase, is often reported by many authors. Based on Eqns. (1), (2a) and (2b), the relative fractions of the electroactive β and γ phases for all samples in the main article are calculated (**Tab. S2)**. Assuming that there are at most three phases (α, β and γ) in all samples, the relative fraction of the nonelectroactive α phase, $F(\alpha)$, can be therefore calculated by using $F(\alpha) = 1 - F_{EA}$. It is found that all samples at least contain two phases, of which the α phase normally exists. A very high fraction of the γ phase, namely 99.3%, was obtained for sample in Fig. 4(B)-curve b, while a lower but still comparatively high fraction of the β phase, namely 94.3%, was for sample in Fig. 3(C)-curve c.

Tab. S2 Percentages of the α, β and γ phases in Figs (2-6)

Samples in	$F(\alpha)$%	$F(\beta)$%	$F(\gamma)$%
Fig. 2(B)	87.8	12.2	0
Fig. 3(Ca)	86.8	13.2	0
Fig. 3(Cb)	7.0	0	93.0
Fig. 3(Cc)	0.4	94.3	5.3
Fig. 4(Ba)	87.1	12.9	0
Fig. 4(Bb)	0.7	0	99.3
Fig. 4(Bc)	0.5	85.6	13.9
Fig. 5(a)	56.4	43.6	0
Fig. 5(b)	43.4	0	56.6
Fig. 5(c)	18.4	53.9	27.7
Fig. 5(d)	28.5	34.0	38.5
Fig. 6(a)	2.2	9.7	88.1
Fig. 6(b)	1.7	55.4	42.9
Fig. 6(c)	0.8	66.8	32.4
Fig. 6(d)	2.9	77.8	19.3

References

[1] S. K. Ghosh, M. M. Alam, and D. Mandal, *RSC Adv*. 2014, **4**, 41886-41896.

[2] M. Kobayashi, K. Tashiro and H. Tadokoro, Macromolecules, 1975, **8**, 158-171.

[3] Boccaccio, T., Bottino, A., Capannelli, G., Piaggio, P., J. Membr. Sci., 2002, **210**: 315-329.

[4] Bormashenko, Y., Pogreb, R., Stanevsky, O., Bormashenko, E., Polym. Test., 2004, **23**: 791-796.

[5] G. Zhong, L. Zhang, R. Su, K. Wang, H. Fong and L. Zhu, Polymer, 2011, **52**, 2228-2237

[6] T. Lei, X. Cai, X. Wang, L. Yu, X. Hu, G. Zheng, W. Lv, L. Wang, D. Wu, D. Sun and L. Lin, RSC Adv., 2013, **3**, 24952-24958.